Land Cover Classification in the Poyang Lake Region, China, Using Landsat TM and JERS-1 Synthetic Aperture Radar Data

Huiyong Sang[1 2], Hui Lin[1], Limin Yang[3], Ying Liu[3], Xiangming Xiao[2]

[1]Institute of Space and Earth Information Science, The Chinese University of Hong Kong, Hong Kong, China
[2]Institute for the Study of Earth, Oceans and Space, University of New Hampshire, Durham, NH 03824, USA
[3]Key Lab of Poyang Lake Ecological Environment and Resource Development, Jiangxi Normal University, Nanchang, Jiangxi Province, China
E-mail: sanghuiyong@cuhk.edu.hk

Abstract
The Poyang Lake is the largest fresh water lake in China. As an internationally important wetlands, conservation of wild birds needs updated information on land use and land cover in the Poyang Lake region. This paper introduced a non-parametric knowledge-based classification method (decision tree classifier) for land cover classification in the Poyang Lake region. We merged optical sensor (Landsat 5 TM) image with Japanese Earth Resource Satellite-1(JERS-1) synthetic aperture radar (SAR) images. The overall accuracy of the classification result was about 82%, of which forest was classified with higher accuracy (over 87%) and less errors of omission and commission. Main classification errors came from the similar spectrum of different land cover classes in winter. The seasonal dynamics should be considered for selecting optical satellite images for classification when using this pixel-based classification algorithm. The results of this study suggests that the non-parametric decision tree classifier together with fusion of optical and SAR images is an efficient method for mapping complex landscapes with agriculture, wetlands and forests.

Keywords
Decision tree classification method, Poyang lake, Remote sensing, JERS-1 SAR

I. INTRODUCTION

Land use changes are cumulatively transforming land cover at an accelerating pace on global scale(Turner, et al., 1994). Land use/cover changes in terrestrial ecosystems are closely linked with the issue of sustainability of socio-economic development since they affect essential parts of our natural capital such as climate, soils, vegetation, water resources and biodiversity (Mather, et al., 1991). It was widely recognized that land use change is a major driver of global change, through its interaction with climate, ecosystem processes, biogeochemical cycles, biodiversity and human activities(Lambin, et al., 1999). Therefore, land cover mapping is important and necessary for quantifying past land use changes, modeling the processes of biogeochemical cycles, and predicting the effects of land use changes on the dynamics of land cover in the near future.

The Poyang Lake is now the largest fresh water lake in China and covers over 4000 square kilometers. It plays an important role in regional water resource management and biodiversity. However, due to the reclamation of natural wetlands and urban development since last mid-century, main lake area reduced over 2000 square kilometers. Many rivers were filled up and their flow directions were even altered. The reduction of water holding capacity in the Poyang Lake caused great loss to local people during the historically largest flood event in 1998. Quantifying the areas of individual land cover types during this period is necessary in order to study the driving factors of flooding and make policies of land-use conversion after this big flood disaster.

Optical remote sensing techniques have proven efficient for land cover and classification in the past 20 years. The vegetation indices were derived from Advanced Very High Resolution Radiometer (AVHRR) images, including Normalized Difference Vegetation Index (NDVI), Seasonally-Integrated Normalized Difference Vegetation Index (SINDVI), Soil Adjusted Vegetation Index (SAVI) and Vegetation Health Index (VHI); and these vegetation indices were widely used to map seasonal or interannual dynamics of vegetation(Hope, et al., 2003; Pelkey, et al., 2003; Boken, et al., 2004; Ferreira, et al., 2004). Other applications of vegetation indices include: NDVI for monitoring mangrove in east coast of India using IRS-1C LISS3 images(Satyanarayana, et al., 2001), Modified NDVI (MNDVI) and Modified SAVI (MSAVI) in Brazilian Amazon using SPOT-4 Vegetation data(Carreiras, et al., 2003) and NDX model for unmixing coast marsh using TM images(Rogers, et al., 2004). TM images were also used to map mammalian habitat and biological diversity in Maasai Mara ecosystem based on the integration of remote sensing and GIS(Oindo, et al., 2003). Mason and others(Mason, et al., 2003) used airborne LiDAR data to measure skylark habitat variables for organism-habitat models.

However, clouds and rains hampered the acquisition of multi-temporal optical remote sensing data from such optical sensors like Landsat and SPOT-4, and thus few multi-temporal images are available for land cover classification. Microwave remote sensing technique has all-day and all-weather capacity in monitoring and mapping the earth, and is sensitive to soil moisture content and vegetation structure, an advantage over optical sensors. Integration of optical images with microwave remote sensing data has been adopted in mapping specific land cover types or changes. Multi-temporal AVHRR and

1082-4006/07/13(01-02)-36$5.00

RADARSAT imagery were used to monitor flood extent in the Northeast China(Zhou, et al., 2000). The synergy of airborne hyperspectral and radar imagery was used to map tropical mangrove ecosystems in coastal area of Australia(Held, et al., 2003). The overall accuracies in discriminating different vegetation types were slightly improved by integrating time series of ERS-1 data and SPOT XS image, compared with the results generated only using ERS-1 images or optical images (SPOT XS and Landsat TM imagery)(Chust, et al., 2004).

The classification and regression tree (CART) algorithm produces rule-based models for prediction of discrete/ continuous variables based on training data. Unlike neural network, the tree developed by this algorithm is interpretable and easy to use. This algorithm has been used to predict and map continuous variables such as tree canopy coverage and imperious surface(Huang, et al. 2001, Yang, et al. 2003a, Homer, et al. 2004) using Landsat-7 Enhanced Thematic Mapper plus (ETM+) imagery over large areas. In this study, the decision tree classifier, one approach of CART, was introduced to map categorical(discrete) variables- land cover types through integrating multi-temporal JERS-1 images with a Landsat 5 TM image to generate the land cover map in the Poyang Lake region.

II. STUDY AREA

The Poyang Lake in Jiangxi Province covers an area of more than 4000 square kilometers (Figure 1), and it plays an important role in regional flooding control and water resource management. Five rivers(Gangjiang, Xiushui, Raohe, Xinjiang and Fuhe) flow into different parts of the Poyang Lake. As it is connected to downstream Yangtze River, the flooding pattern of the Poyang Lake was influenced not only by local precipitation and water source from the five rivers, but also by the backflows from Yangtze River. Thus, the flooding pattern in the lake varies from area to area and from year to year.

The study area is located in middle part of the Poyang Lake region, within 28°43'~29°8' N and 115°50'~116°37' E (Figure 1). The land cover types in this region include water body, herbaceous vegetation in wetlands around open water, bog, sandy area, residential area, trees and shrub in uplands, and agriculture. Natural wetlands are colonized by floating vegetation, submergent vegetation, emergent *Carex* community, and emergent semi-aquatic higher plant (*Miscanthus floridulus & Phragmites communis*) community, from open water to lake peripheries with the variation of elevation and environment conditions. Agricultural systems are dominated by single rice cultivation system and rice-rice rotation system; rapeseed-rice rotation system also exists depending on local soil and weather condition.

Subtropical monsoon climate causes distinct dry and rainy seasons in the Poyang Lake region. The rainy season starts in early April when southeast monsoon starts to influence this

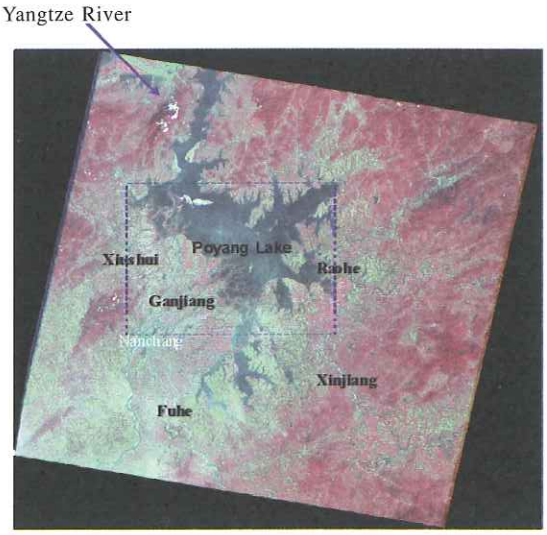

Figure 1. The study area in the Poyang Lake region, Jiangxi Province, China. Landsat TM image acquired on December 10, 1999 was displayed here, a false color composite of band 4 (red), band 3(green) and band 2(blue)

region. Precipitation in the rainy season gradually decreases as summer monsoon retreats after July, and then the dry season follows with less precipitation. Annual precipitation is approximately 1482mm, but precipitation varies significantly between months, years, and even different parts of the Poyang Lake region. Maximum monthly precipitation occurs in June, accounting for over 17% of annual precipitation, whereas minimum monthly precipitation in December is only 42mm. Influenced by both summer and winter monsoons, distinct four seasons (spring, summer, fall and winter) also exist in this region with very hot weather in summer and cold weathers in winter. Annual mean temperature is about 25°C, with highest monthly average temperature in July (29.4°C) and lowest in January (4.8°C)(Zhu, 1997).

The data of water level dynamic in 1998 were collected at the Tangyin hydrological station (Figure 2). In 1998 one of the historical biggest floods took place along the Yangtze River watershed including the Poyang Lake region. The highest water level observed at the Tangyin hydrological station was 22.57 m on July 30, in 1998. The flooding lasted almost four months from June to September when water level depth was keeping above 20 m, and caused significant loss and damages to local people and society.

III. SATELLITE DATA

Landsat 5 Thematic Mapper (TM) image on Dec 10th, 1999, and multi-temporal high resolution Japanese Earth Resources Satellite-1 (JERS-1) Synthetic Aperture Radar (SAR) intensity images from the end of 1997 to summer in 1998 were obtained for this study (Table 1). JERS-1 SAR sensor operated at 1.3G L band in HH polarization, and one high resolution image covered about 75 km width with the resolution of 18-m. JERS-1 raw

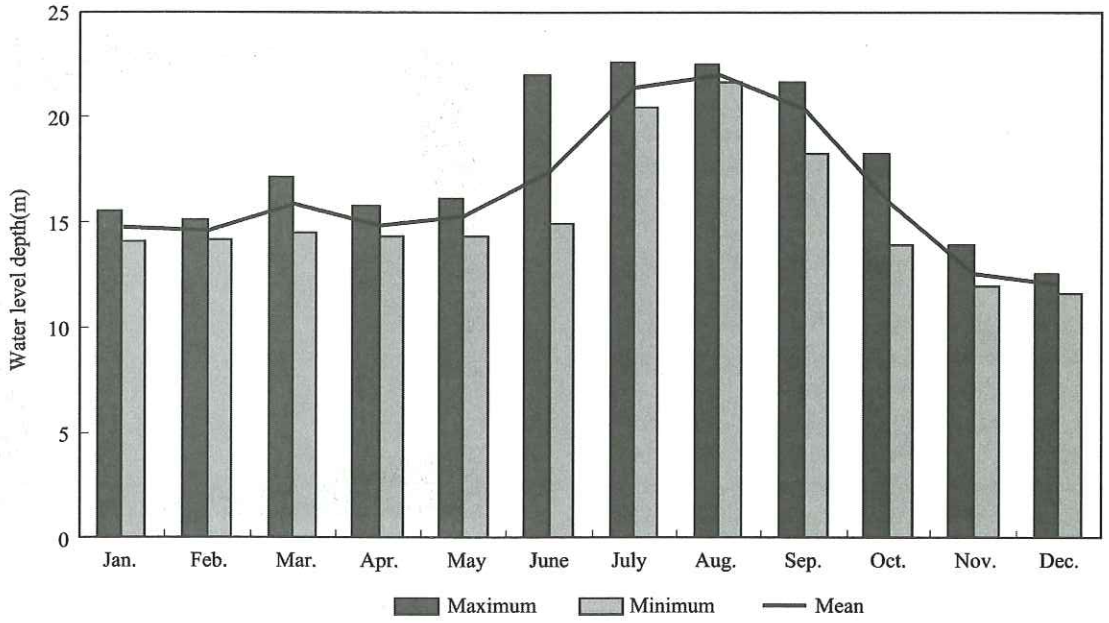

Figure 2. Seasonal dynamics of water level observed at Tangyin hydrological station

Table 1. Satellite images used in this study for land cover classification

Satellite data	Date
Landsat 5 TM	December10th, 1999
JERS-1	December 6th, 1997
JERS-1	January 29th, 1998
JERS-1	April 27th, 1998
JERS-1	June 10th, 1998
JERS-1	July 24th, 1998

data were input to GAMMA Modular SAR Processor (MSP) to generate multi look intensity SAR imagery data with the pixel size of 15m×15m (http://www.gamma-rs.ch/). All these intensity images were geo-corrected and co-registered with the projection of UTM WGS84 in GAMMA SAR Geocoding and Image Registration Software (GEO), using the Shuttle Radar Topography Mission (SRTM) 90 m DEM data downloaded from USGS EROS data center (http://edc.usgs.gov/). Gamma Map filtering was applied to reduce the speckles within the 5×5 window in PCI 10.0 software package. The Landsat 5 TM image was co-registered to JERS-1 data and resampled to the same pixel size.

IV. METHODOLOGY

The decision tree classification algorithm for land cover classification through integrating multi-source remote sensing data is a supervised classification method. The training data are first selected as input for learning and training to construct a decision tree model, which should preliminarily be evaluated. After applying the model spatially, the training data may need to be modified based on the intermediate classification map. The decision tree model would be re-constructed if necessary (Figure 3).

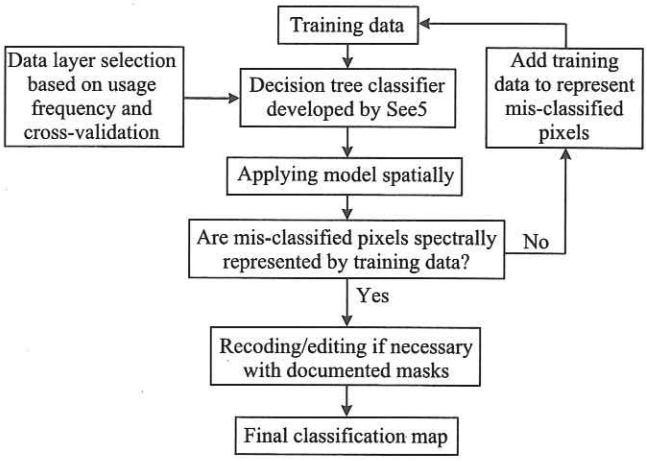

Figure 3. The schematic diagram of land cover classification procedure in this study

A. Decision tree classifier

Decision tree classifier is a machine learning algorithm, which conducts a binary recursive partitioning and generates a set of if-then rules based on training data to predict a target variable (Yang, et al., 2003b). As a non-parametric classifier, the decision tree algorithm can handle a mixture of nominal, ordinal and quantitative data types, without necessity to consider the statistic distribution of training data(Gahegan, et al., 1998). The decision tree classifier used in this study was developed

using the software See5/C5 (*http://www.rulequest.com/see5-win.html#CLASSIFIERS*), and it recursively uses a gain ratio criterion in generating a decision tree from a set of training data. The complex tree constructed in See5/C5 could be simplified and become more comprehensible by discarding one or more subtrees and replacing them with leaves using an error-based pruning method at a given confidence level (Quinlan, 1993). The software See5/C5 could also pre-select a subset from an abundance of attributes for constructing a decision tree or rule-sets in order to reduce data redundancy. Another advanced feature of the See5/C5 is its ability to estimate the predictive accuracy by N-fold cross-validation. In this option, the training data are divided into n blocks of almost equal size and uniform class distribution. For each block (hold-out block) in turn, a classifier is built from the remaining blocks and tested using the hold-out block. The average error rate over the n classifiers is the final accuracy of the decision tree (http://www.rulequest.com/see5-win.html#XVAL).

B. Training and test data collection

The strongest limiting factor in the decision tree classifier lies in how carefully the target classes are chosen and how well the attributes of the target classes are characterized (Gahegan, et al., 1998). The Level-1 land cover classes for studying the interactions between the atmosphere, the biosphere and soils at global scale include water, wetlands, bare soil, agriculture, grassland, shrubland, savanna, deciduous forest, coniferous forest, evergreen broadleaf forest, and urban areas(Dobson, et al., 1996). The topography around the Poyang Lake is very complex, and includes mountains, hills to floodplain. Natural wetlands are a dynamic system, and its coverage fluctuates with open water area as water level changes over time. Most croplands surrounding the lake are reclamation fields from natural wetlands, and grow rice, rapeseed, peanuts and other crops. Hills or uplands are covered with grass, shrubs and forests. Considering local land cover attributes around the Poyang lake region, we define a land cover classification scheme with 7 classes: water, wetlands, bare land, cropland, forest, urban/residential area and shrubs. Training data representing above seven land cover classes were visually picked up from Landsat5 TM image as shown in Table 2. Input attributes of the training data for developing a decision tree classifier includes seven Landsat 5 TM bands and five scenes of JERS-1 images as listed in Table 1.

C. Model validation and input data layer selection

The decision tree algorithm is a knowledge-based data mining method, and it is sensitive to the distribution of training data. Thus the training data representing certain classes would be modified through checking the classification map after n-fold cross validation to generate a preliminary error matrix based on training data or applying it spatially to the whole area. That is to say, if one land cover class was overestimated or underestimated, some of the training data representing it should be deleted from or added to this class; if two classes were mixed or misclassified with each other, the training data quality representing them should be checked again or sometimes more data be added.

Table 2. Sample sizes (number of pixels) of training data sets for different land covers in this study

Land cover	Training data
Bare soil	63
Cropland	648
Forest	318
Shrub & grassland	408
Urban and Residential	357
Water	150
Wetlands	396

Although twelve data layers were input for constructing the decision tree classifier, the 4 layers including TM band 1 and band 7, JERS-1 images on December 6th 1997, and April 27th 1998 were found to be negligible and winnowed in final decision tree development, after evaluating their contribution to decision tree development. The importance of input data layers through calculating their usage frequency for one class was also listed in Table 3. Most land cover classes were differentiated by TM band 4 and band 2. Although upper data layers are generally less important, they are very significant for specific classes. For instance, TM band 3 was the most important attribute for separating forest, but it made ignorable contribution to the classification of cropland and water. The same situation happened to JERS-1 on January 29th and June 10th, 1998 for water, and TM band 3 for bare land.

V. ACCURACY ASSESSMENT

After modifying training data several times, the final decision tree model was constructed and applied spatially to generate a preliminary classification map. Although cross-validation can give an evaluation about the effect of classification model based on training data, a more objective accuracy assessment process was given through randomly creating test points. The error matrix of accuracy assessment for the preliminary classification map is given in Table 4, and the overall accuracy is about 80% and Kappa statistics is 0.8. The greatest error of commission occurs on "urban/residential area", with user's accuracy of about 60% and Kappa statistics of 0.6. About 10% of the bare land and water area were misclassified to urban/residential area. The residential areas were mostly villages or small towns, where no high-density and tall buildings existed. Both mudflat and sand either emerged above water surface or was covered with very shallow water in winter. However, training data representing water class were still picked from these areas because they would be flooded before wetland vegetation sprouts. As shown in Table 3, the dominant attributes for separating these seven land cover classes were

Table 3. Utilization and contribution of individual data layers to decision tree construction

	Bare soil		Cropland		Forest		Shrubby grassland		Residential area		Water		Wetland		Average importance (%)
	Using frequency	Importance (%)	Using frequency	Importance (%)	Using frequency	Importance (%)	Using frequency	Importance (%)	Using frequency	Importance (%)	Using frequency	Importance (%)	Using frequency	Importance (%)	
Jers1980129	0	0	26	1	58	4	40	2	119	**16**	151	**24**	3	0	**3**
Jers1980610	0	0	81	2	2	0	7	0	3	0	149	**23**	170	9	**3**
TM band 5	0	0	81	2	7	0	219	10	17	2	6	1	223	**12**	**7**
TM band 6	3	1	616	13	62	4	66	3	8	**1**	6	1	31	2	**7**
TM band 3	59	**23**	106	2	606	**37**	331	15	17	2	0	0	160	9	**11**
Jers1980712	0.0	0	624	13	324	**20**	358	16	129	17	6	1	235	13	**14**
TM band 2	71	27	1775	38	317	19	437	20	193	**25**	161	25	393	22	**28**
TM band 4	127	49	1323	29	251	15	713	33	271	**36**	161	25	579	32	**29**

Table 4. Error matrix for accuracy assessment of land cover classification

	bare land	cropland	forest	shrubs	urban/resid.	water	wetlands	total	user's accuracy (%)
Bare land	48	2	0	0	0	0	0	50	96
cropland	17	77		2	2	4	11	113	68
forest	0	2	47	4	0	0	1	54	87
shrubs	0	3	6	43	3	0	5	60	72
urban/resid.	8	4	0	0	34	9	0	55	62
water	1	2	0	0	0	95	1	97	98
wetlands	0	1	0	0	0	0	70	71	99
total	74	88	53	49	39	109	88	500	
producer's accuracy(%)	65	88	89	88	87	87	80		83
Kappa	0.9531	0.6134	0.8550	0.6859	0.5859	0.9736	0.9829	0.7968	

TM band 2 and band 4 in winter. The surface reflectance values of urban/residential area and mudflats are very close and difficult to be separated. Another overestimated class was "cropland", which has user's accuracy of 68% and Kappa statistics of 0.61. In winter season, most croplands were fallow and covered with grass or residual rice stalks, which were easily mixed with bare land. Also the surface reflectance of withered wetland vegetation was similar with that of crops growing in winter. Thus bare land was mapped with the most significant errors of omission. Another error resource was from visual interpretation for training data collection and accuracy assessment, which were carried out using Landsat 5 TM image. Topographical relief and cropland patches distributed among hills resulted in mixed pixels in Landsat TM image at 30-m spatial resolution.

VI. RESULTS

77 field samples including land cover types and geographic locations were collected in 2005 and 2006, of which 41 samples from wetlands, 17 from cropland, 9 from urban/residential area and 1 from shrubs were correctly mapped (Table 5). However, among the 15 samples from cropland, 4 were collected from those short (less than 10cm) and low-density grassland mixed with bare land. 9 samples of bare land were misclassified to

Table 5. Field samples for validating the classification results in this study

Map	Field				total
	wetlands	cropland	urban/resid.area	shrubs	
wetlands	36				36
cropland	5	24	3		32
urban/resid. area			6		6
shrubs		2		1	3
total	41	26	9	1	77

cropland, because these samples were mainly collected from soil roads among croplands mixed with grass along roadsides. The width of these country roads are mostly less than 1 pixel size (15m) and are easily mixed with cropland. Also 3 samples from urban/residential areas were misclassified to cropland, which might be attributed to land cover changes between 1999 and 2006. Two samples from cropland were misclassified to shrubs, where rapeseeds were grown in the winter of 2005–2006. As shown in Table 3, the land cover map was determined by band 2 and band 4 of the TM image. Most croplands near Poyang Lake were grown single or double harvesting rice and kept fallow in winter, and the spectrum of croplands were similar to that of short grassland. Thus the mapped croplands should include grasslands. However, the spectrum of rapeseeds was similar to that of shrubs in winter. Natural wetlands were mostly mapped correctly, but still 4 samples from wetlands were mixed with croplands.

The preliminary classification map was generated only using the decision tree developed in See5/C5, without any post-classification processes that introduce other knowledge or data layers. After manually editing the obviously misclassified areas near water area and wetlands through visual interpretation, the final land cover map is shown in Figure 4.

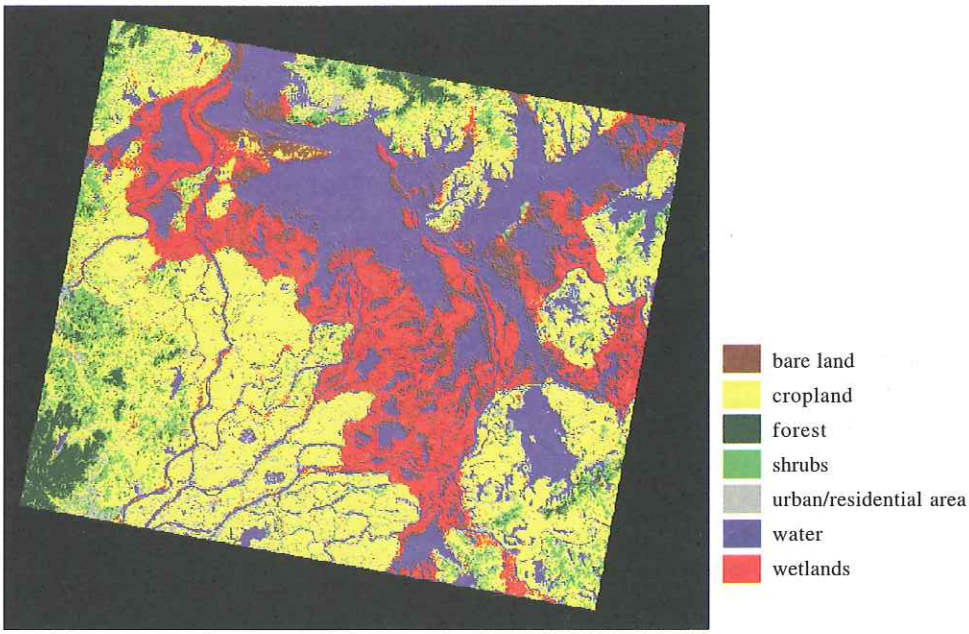

Figure 4. Land cover map of the Poyang Lake region, China, in 1998

The entire study area covered about 5711 square kilometers. Open water body accounted for 28.6%. Open water area varied from month to month and year to year, depending on local precipitation and water flow from the rivers in the region (Figure 1). In this study, floating vegetation under water surface could not be detected by TM or JERS-1 images. Those areas colonized by aquatic and semi-aquatic emergent vegetation (defined as wetlands), covered about 850 km^2. The mudflats, which generally covered by water except in winter, were mostly classified as open water areas, and a small partion of mudflats were classified as bare land. Cropland has the largest area in the Poyang Lake region, and covered over 2000 km^2. Most croplands were reclaimed from previous natural wetlands. Reclamation of wetlands and overly land use were the two factors that contribute to the largest flood and substantial loss in 1998.

Forests in mountainous areas and shrubs mixed with grass in uplands accounted for 180km^2 and 400km^2 respectively. In the study area, only part of Nanchang city is included, and there are no other large cities. These small towns and villages covered about 260 km^2. The sandy bare surface close to natural wetlands and water body has an area of about 350km^2. Some of reclaimed croplands were returned to natural wetlands or lakes after the big flood in 1998. Some towns or villages near natural wetlands were severely damaged by the flood and were then abandoned, and local people moved to other places.

VII. DISCUSSION AND CONCLUSION

A machine auto-learning decision tree classifier was used in this study to conduct land cover classification. Optical remote sensing image was fused with JERS-1 SAR images as input to the decision tree classifier. The optical TM image dominated the classification result, and the JERS-1 SAR images were only complementary in this algorithm. The classification error of cropland was mainly attributed to similar surface reflectance values among harvested croplands, bare land and wetlands in winter. The high accuracy in identifying natural wetlands was partly ascribed to the JERS-1 image acquired on July 12, 1998, when most wetlands were flooded due to high water level. Seasonal dynamics of individual land cover types should be considered when acquiring remote sensing data in land cover

classification, especially for those land cover types with high seasonal dynamics, for instance agriculture and wetlands.

Corner reflection in urban/residential areas resulted in high backscattering signals which would make it easy to distinguish buildings from other land cover types using radar images. However, the superiority of SAR image in classifying urban/residential area over optical imagery was not displayed in this study, and it was instead weakened by integrating both of them. The similar spectrum of urban/residential areas with low density buildings to shallow water is the major reason for the commission error in urban/residential areas.

The ability of L-band HH-polarized JERS-1 SAR data in land-use/land-cover mapping has been proven due to its deep penetration ability and higher sensitivity to vegetation structures(Dobson, et al., 1996; Angelis, et al., 2002; Freeman, et al., 2002; Rosenqvist, et al., 2002). However, because the time series of JERS-1 images processed by GAMMA were not standard products, these intensity images could not be calibrated to normalized backscatter coefficients(Salas, et al., 2002). The thresholds used in the decision tree models from the intensity images were not comparable before normalization, which resulted in some difference on the classification results. Thus, the potential of the time series JERS-1 data in separating residential area and vegetations with different structures were not fully explored in this study, even though forest and wetland vegetation were mapped with higher accuracy.

Higher resolution image or field samples from homogeneous targets should be used when selecting training data to avoid those mixed pixels of two or more land cover types, especially for shrubs and croplands. Generally, this non-parametric classification algorithm has great potential in land cover classification and the result can be improved significantly if the optical remote sensing images in other seasons and the normalized backscatter coefficients of JERS-1 imagery were available .

ACKNOWLEDGEMENT

We thank Dr. Zhong Lu at USGS for providing JERS1 images. This study was supported by the Key Lab of Poyang Lake Ecological Environment and Resource Development, Jiangxi Normal University.

REFERENCES

[1] Turner II B L., W. B. Meyer, D. L. Skole, 1994, Global Land-Use Land-Cover Change-Towards an Integrated Study. Ambio 23: 91–95.

[2] Mather J R., G. V. Sdasyuk, 1991, Global change: geographical approaches. University of Arizona Press, Tucson.

[3] Lambin E F., X. Baulies, N. Bockstael, G. Fischer, T. Krug, R. Leemans, E. F. Moran, R. R. Rindfuss, Y. Sato, D. Skole, B. L. Turner II, C. Vogel, 1999, Land-Use and Land-Cover Change (LUCC): Implementation Strategy. IGBP report 48 and IHDP report 10.

[4] Hope A S., W. L. Boynton, D. A. Stow, D. C. Douglas, 2003, Interannual growth dynamics of vegetation in the Kuparuk River watershed, Alaska based on the Normalized Difference Vegetation Index. International Journal of Remote Sensing, 24: 3413–3425.

[5] Pelkey N W., C. J. Stoner, T. M. Caro, 2003, Assessing habitat protection regimes in Tanzania using AVHRR NDVI composites: comparisons at different spatial and temporal scales. International Journal of Remote Sensing, 24: 2533–2558.

[6] Boken V K., G. Hoogenboom, F. N. Kogan, J. E. Hook, D. L. Thomas, K. A. Harrison, 2004, Potential of using NOAA-AVHRR data for estimating irrigated area to help solve an inter-state water dispute. International Journal of Remote Sensing, 25.

[7] Ferreira L G., A. R. Huete, 2004, Assessing the seasonal dynamics of the Brazilian Cerrado vegetation through the use of spectral vegetation indices. International Journal of Remote Sensing, 25: 1837–1860.

[8] Satyanarayana B., B. Thierry, D. Lo Seen, A. V. Raman, G. Muthusankar, 2001, Remote sensing mangrove research-relatiohship between vegetation indices and dendrometric parameters: a case for Coringa, east coast of Indina. 22nd Asian Conference on Remote Sensing, 5–9 November 2001, Singapore.

[9] Carreiras J M B., J. M. C. Pereira, Y. E. Shimabukuro, D. Stroppiana. 2003. Evaluation of compositing algorithms over the Brazilian Amazon using SPOT-4 VEGETATION data. International Journal of Remote Sensing, 24: 3427–3440.

[10] Rogers A S., M. S. Kearney, 2004, Reducing signature variability in unmixing coastal marsh Thematic Mapper scenes using spectral indices. International Journal of Remote Sensing, 25: 2317–2335.

[11] Oindo B O., A. K. Skidmore, P. De Salvo, 2003, Mapping habitat and biological diversity in the Maasai Mara ecosystem. International Journal of Remote Sensing, 24: 1053–1069.

[12] Mason D C., G. Q. A. Anderson, R. B. Bradbury, D. M. Cobby, I. J. Davenport, M. Vandepoll, J. D. Wilson, 2003, Measurement of habitat predictor variables for organism-habitat models using remote sensing and image segmentation. International Journal of Remote Sensing, 24: 2515–2532.

[13] Zhou C H., J. C. Luo, C. J. Yang, B. L. Li, S. L. Wang, 2000,Flood monitoring using multi-temporal AVHRR and RADARSAT imagery. Photogrammetric Engineering and Remote Sensing, 66: 633–638.

[14] Held A., C. Ticehurst, L. Lymburner, N. Williams, 2003, High resolution mapping of tropical mangrove ecosystems using hyperspectral and radar remote sensing. International Journal of Remote Sensing, 24: 2739–2759.

[15] Chust G., D. Ducrot, J. L. L. Pretus, 2004, Land cover discrimination potential of radar multitemporal series and optical multispectral images in a Mediterranean cultural landscape. International Journal of Remote Sensing, 25: 3513–3528.

[16] Huang C., L. Yang, B. Wylie, C. Homer, 2001, A Strategy for Estimating Tree Canopy Density Using Landsat 7 ETM+ and High Resolution Images over Large Areas. *in* the Third International Conference on Geospatial Information in Agriculture and Forestry, Denver, Colorado, USA.

[17] Yang L M., C. Q. Huang, C. G. Homer, B. K. Wylie, M. J. Coan. 2003a. An approach for mapping large-area impervious surfaces: synergistic use of Landsat-7 ETM+ and high spatial resolution imagery. Canadian Journal of Remote Sensing, 29: 230–240.

[18] Homer C., C. Q. Huang, L. M. Yang, B. Wylie, M. Coan, 2004, Development of a 2001 National Land-Cover Database for the

United States. Photogrammetric Engineering and Remote Sensing, 70: 829–840.

[19] Zhu H., B. Zhang, 1997, Poyang Lake (*in chinese*). the University of Science and Technology of China Press, Hefei.

[20] Yang L M., G. Xian, J. M. Klaver, B. Deal. 2003b. Urban land-cover change detection through sub-pixel imperviousness mapping using remotely sensed data. Photogrammetric Engineering and Remote Sensing, 69: 1003–1010.

[21] Gahegan M., G. West, 1998, The classification of complex geographic datasets: an operational comparison of artificial neural network and decision tree classifiers. *in* the 3rd International Conference on GeoComputation, University of Bristol, United Kingdom.

[22] Quinlan J R, 1993, C4.5 programs for machine learning. Morgan Kaufmann Publishers, San Mateo, California, USA.

[23] Dobson M C., L. E. Pierce, F. T. Ulaby, 1996, Knowledge-based land-cover classification using ERS-1/JERS-1 SAR composites. IEEE Transactions on Geoscience and Remote Sensing, 34: 83–99.

[24] Angelis C F., C. C. Freitas, D. M. Valeriano, L. V. Dutra, 2002, Multitemporal analysis of land use/land cover JERS-1 backscatter in the Brazilian tropical rainforest. International Journal of Remote Sensing, 23: 1231–1240.

[25] Freeman A., B. Chapman, P. Siqueira, 2002, The JERS-1 Amazon Multi-season Mapping Study(JAMMS): Science objectives and implications for future missions. International Journal of Remote Sensing, 23: 1447–1460.

[26] Rosenqvist A., C. M. Birkett, 2002, Evaluation of JERS-1 SAR mosaics for hydrological applications in the Congo river basin. International Journal of Remote Sensing, 23: 1283–1302.

[27] Salas W A., M. J. Ducey, E. Rignot, D. Skole, 2002, Assessment of JERS-1 SAR for monitoring secondary vegetation in Amazonia: II. Spatial, temporal, and radiometric considerations for operational monitoring. International Journal of Remote Sensing, 23: 1381–1399.